Electronic Supplementary Material (ESI) for Journal of Materials Chemistry B.

SUPPORTING INFORMATION

Seed-mediated synthesis of plasmonic gold nanoribbons using cancer cells for hyperthermia applications

Ajay Vikram Singh*[a], Yunus Alapan[a], Timotheus Jahnke[b], Peter Laux[c], Andreas Luch[c], Amirreza Aghakhani[a], Soheila Kharratiankhameneh[d], Mehmet Cengiz Onbasli[e], Joachim Bill[b], Metin Sitti[a]

[a]Physical Intelligence Department, Max Planck Institute for Intelligent Systems, 70569 Stuttgart, Germany.

[b]Institute for Materials Science, University of Stuttgart, Heisenbergstr. 3, 70569 Stuttgart, Germany.

[c]Department of Chemical and Product Safety, German Federal Institute for Risk Assessment (BfR), Max-Dohrn-Strasse 8-10, 10589, Berlin, Germany

[d]Koç University, Department of Materials Science and Engineering, Sarıyer, 34450 Istanbul, Turkey

[e]Koç University, Department of Electrical and Electronics Engineering, Sarıyer, 34450 Istanbul, Turkey

Supporting Table

Table S1. Physicochemical properties of spherical seeds NPs and 2D nanoribbons

	Mobility (μm cm/s V)	**Zeta Potential (mV)**	**Radius (nm)**
Spherical NPs (seed)	-0.55 ± 0.03	-7.22 ± 0.5	20.1 ± 1.5
2D nanoribbons	-1.13 ± 0.21	-14.68 11	202 ± 13

Supporting Figures

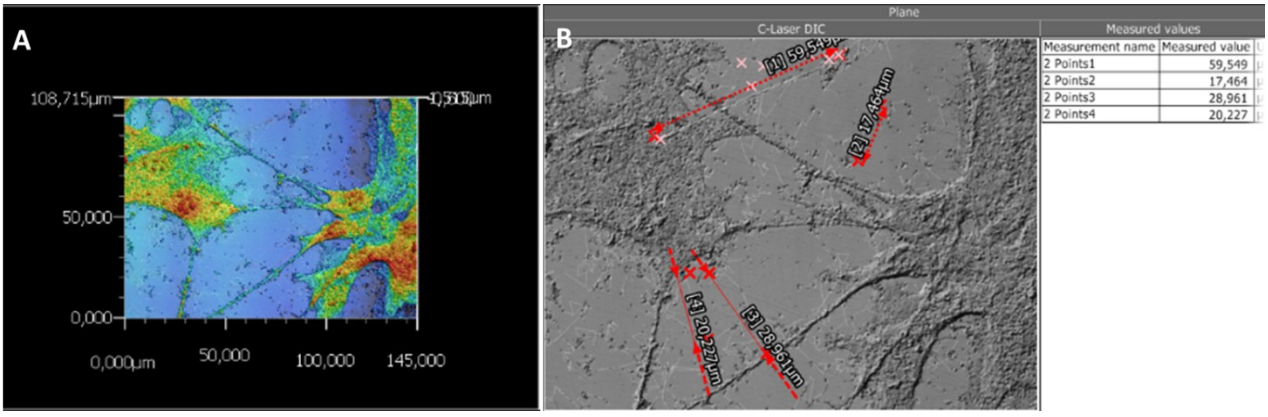

Figure S1. Qualitative and quantitative characterization of surface topography and nanoribbons length/diameter spanning over cell membrane with laser scanning microscopy. (A) 3D topography and (B) optical image of Au-nanoribbon lengths and diameters over mCF7 cells.

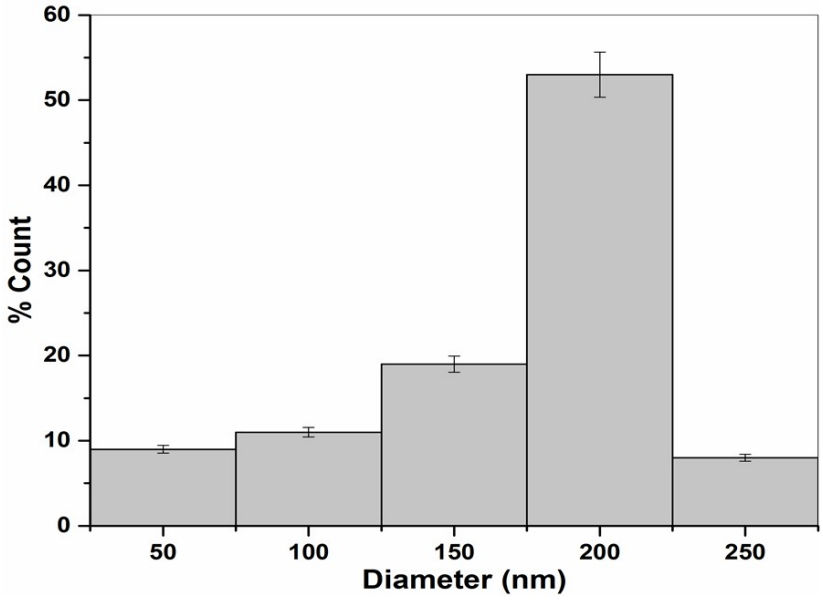

Figure S2. Histogram showing the nanoribbon diameter distribution.

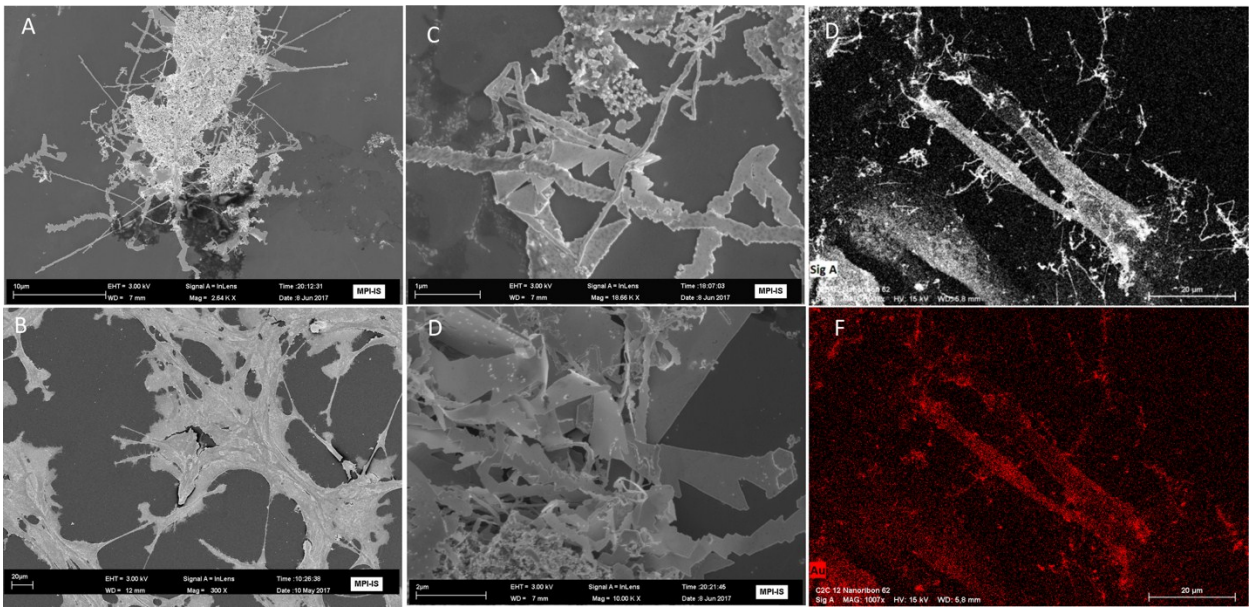

Figure S3. SEM analysis of the influence of gold ion concentration (A-B) versus spherical "seed" NPs concentration on nanoribbon yield. (E-F) elemental mapping and EDAX analysis of nanoribbons.

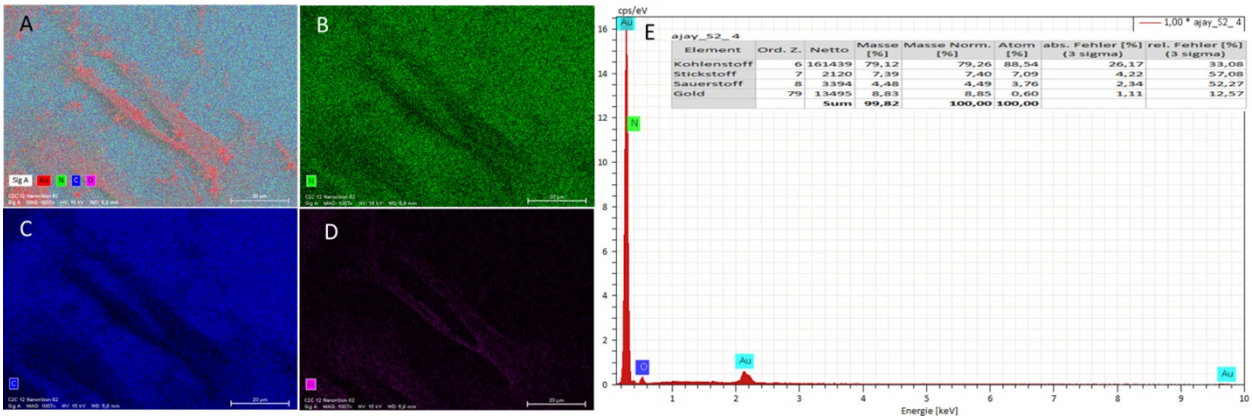

Figure S4. Elemental mapping to demonstrate N, C and O content analysis over the surface of MCF7 cells synthesizing nanoribbons.

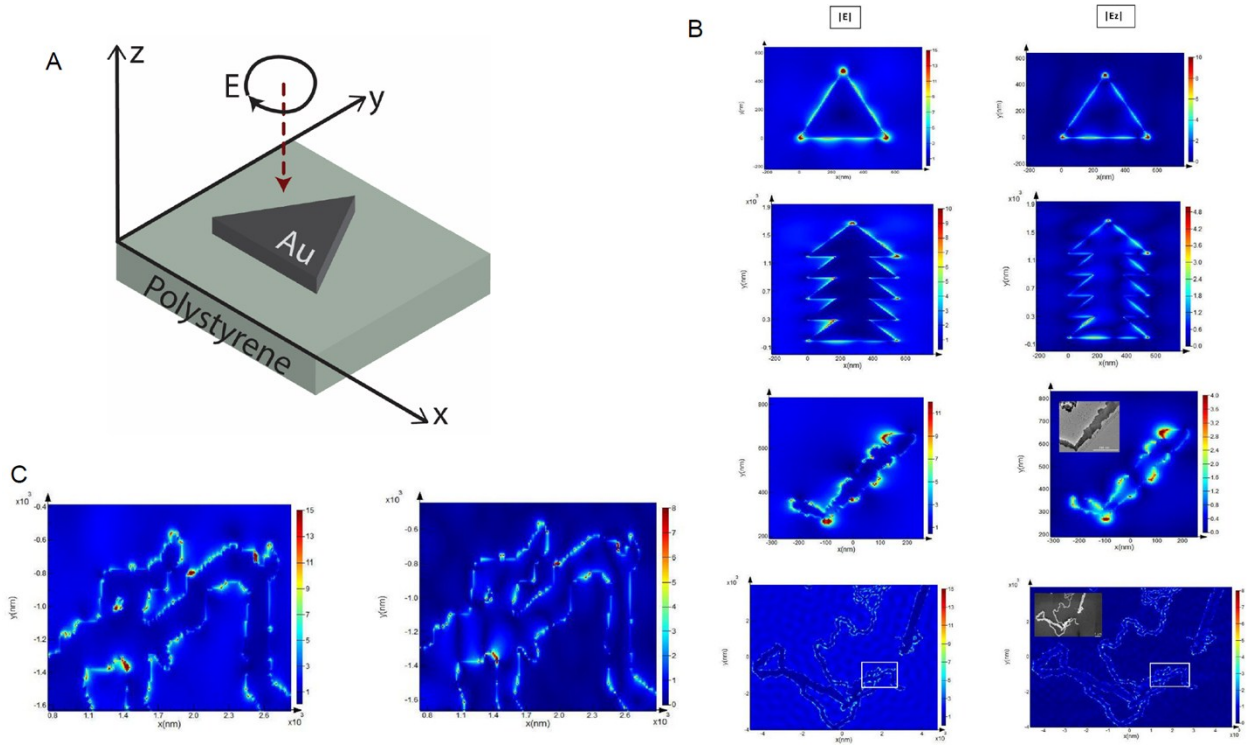

Figure S5. (A) Scheme for computing the propagation constant of wedge-plasmon modes using 3D-FDTD. (B) Energy-filtered images of the triangular nanoplates, fused platelets as a train of nanotriangles and SEM/TEM micrograph. (C) Zoomed version of SEM image with a region of interests (box).

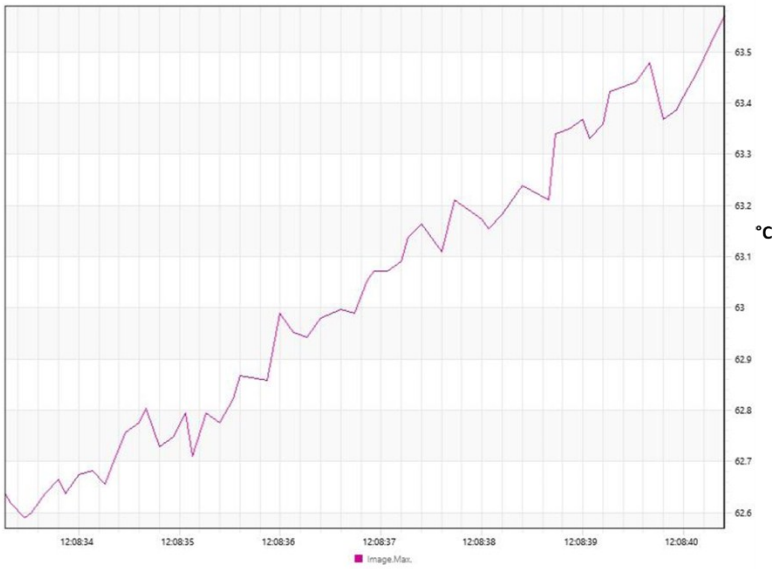

Figure S6. Quantitative line graph extracted from thermograms analyses to show rise in temperature over time.

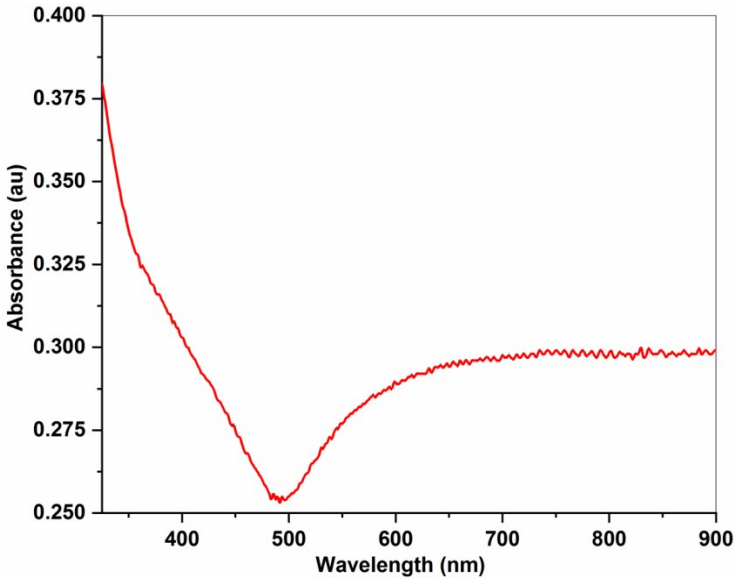

Figure S7. UV-Vis spectra of nanoribbons after purification via centrifugation.

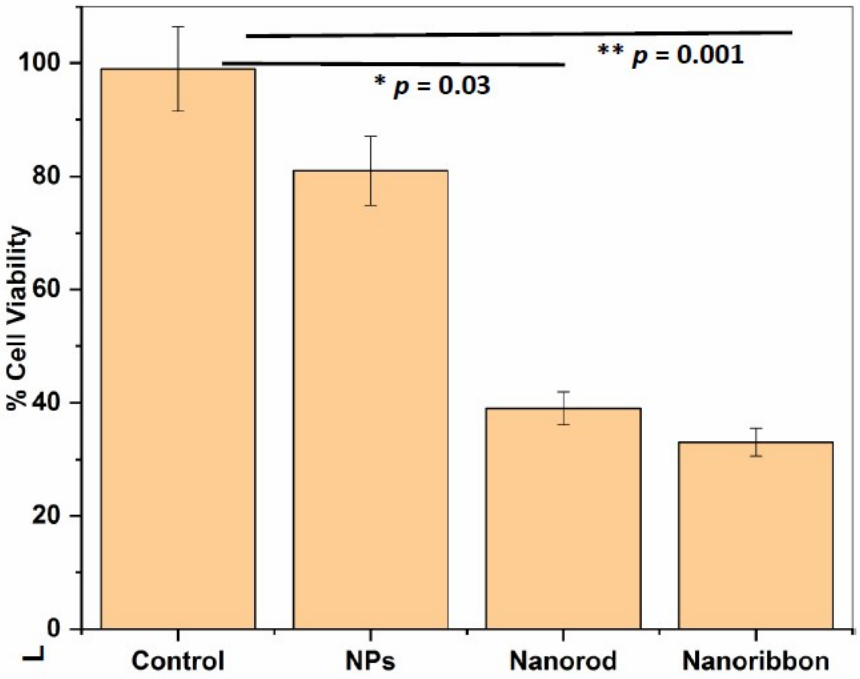

Figure S8. Viable cell quantification after NIR laser irradiation to control experiments and plasmonic nanoribbon treated cancer cells.